Available online at www.sciencedirect.com
SCIENCE DIRECT
ELSEVIER
Polymer 46 (2005) 6532–6542
polymer
www.elsevier.com/locate/polymer

Effect of isothermal crystallization on the amorphous phase mobility of polycarbonate/poly(ε-caprolactone) blends

Estrella Laredo[a,*], Mario Grimau[b], Paula Barriola[b], Alfredo Bello[a], Alejandro J. Müller[b]

[a]*Physics Department, Universidad Simón Bolívar, Apartado 89000, Caracas 1080, Venezuela*
[b]*Materials Sciences Department, Universidad Simón Bolívar, Apartado 89000, Caracas 1080, Venezuela*

Available online 25 May 2005

Abstract

Polycarbonate/poly(ε-caprolatone), PC/PCL, amorphous miscible blends with 90/10 and 80/20 composition in weight, have been studied by X-ray diffraction and broad-band dielectric spectroscopy. The molecular dynamics for the high T_g component segmental mobility have been followed by analyzing the isothermal dielectric losses as a function of frequency with Havriliak–Negami distributions. The PCL plasticization effect is observed as a lowering of the Vogel–Tammann–Fulcher terminal temperature without any significant change in the other relaxation parameters. The isothermal crystallization process of the 90/10 PC/PCL blend has been studied in real time both by following the decrease of mobile amorphous material from the variation of the dielectric losses, and by wide angle X-ray scattering to follow the crystal growth. Quantitative comparisons show the disappearance of much higher amounts of mobile amorphous chains than those that are transferred to the crystallites. The existence of a rigid amorphous phase in the blend is established in non-negligible amounts as the isothermal crystallization of PC develops. The remaining mobile amorphous phase has unchanged dynamics.

Keywords: Polycarbonate crystallization; Rigid amorphous phase; Self-concentrations

1. Introduction

Bisphenol-A polycarbonate/poly(ε-caprolactone), PC/PCL, blends present various compatibility degrees in the amorphous phase as the crystallization degree of the two blend components varies [1,2]. As the composition and temperature change one can encounter semicrystalline–semicrystalline, semicrystalline–amorphous and amorphous–amorphous states. In several previous calorimetric works on this system [3–6] a single dynamic glass transition temperature upon cooling, at intermediate temperatures, has been found. Thus, the existence of a homogeneous mixture of the two polymers in their amorphous phases has been established. However, in a study where the blends were found to be miscible [1] the heat capacity step found in the differential scanning calorimetry, DSC, traces showed an anomalously broadening as the PCL content increased according to the Lodge and McLeish [7] self concentration model prediction's for miscible blends. The model is based on the existence of intramolecular connectivity which affects the composition of the neighborhood of each member's chain of the system. Each component of a miscible blend is surrounded by regions of local composition which differ from the bulk composition. In the system under study, if the PCL amorphous chains are surrounded by regions richer in PCL than the bulk nominal composition, then the dynamics of the low T_g component will show segmental dynamics which should be faster than that of the bulk. For the higher T_g component, PC in our case, the segmental dynamics should be slower than that corresponding to the bulk composition. The length scale relevant to the self-concentration model has been found to be close to the Kuhn segment length [8,9].

A second study [2] on the molecular dynamics of this system by dielectric relaxation techniques, i.e. thermally stimulated depolarization currents (TSDC) complemented by DSC, WAXS (wide angle X-rays scattering), transmission electron microscopy (TEM) and polarized optical microscopy, using slow cooled samples, showed the existence of two well defined TSDC peaks located near the glass transition temperature of each component, together with two calorimetric steps in the DSC traces. These

* Corresponding author. Tel.: +58 212 906 3536; fax: +58 212 906 3527.
E-mail address: elaredo@usb.ve (E. Laredo).

0032-3861/$ - see front matter © 2005 Elsevier Ltd. All rights reserved.
doi:10.1016/j.polymer.2005.05.008

findings were indicative of a phase-separated system where each mixture component shows its own segmental dynamics. Also, the WAXS results showed the crystallization of both PC and PCL in the thermally treated films. The quenched samples where the PC component barely crystallizes, showed very broad relaxation peaks which are indicative of large concentration fluctuations.

TSDC experiments on extruded samples without any further thermal treatment are currently under study and will be published elsewhere. These blends have been found to be miscible in the whole composition range as the DSC traces present a single enthalpic step at intermediate temperatures between the T_g's of the homopolymers. It has also been found that PC is always amorphous and the TSDC spectra presents the two distinct segmental dynamics predicted by Lodge and McLeish [7] for miscible blends in the whole composition range.

In order to study the effect of the PC progressive crystallization on the dynamics of the blend, broad band dielectric spectroscopy, BBDS, experiments were performed on the amorphous neat PC and on the 90/10 and 80/20 PC/PCL blends. First, a series of experiments were carried out as a function of temperature and frequency on extruded samples which showed a single calorimetric T_g. Then, isothermal crystallization of the PC rich blends as a function of time was followed in a dielectric spectrometer and in the high temperature chamber of our X-ray diffractometer. The aim of this work is to gather information on the molecular dynamic changes as the crystal structure develops in an originally amorphous matrix, and on the plasticization effect of the PCL component on the PC. The combined results of the development of crystallinity as seen by WAXS and the disappearance of the amorphous mobile phase followed by BBDS at the same temperatures, should provide a complete overview on the transformations that occur at the chosen temperatures.

2. Experimental section

2.1. Materials

Bisphenol A polycarbonate (PC) (Makrolon 2807) and poly(ε-caprolactone) (PCL) (Tone P787) homopolymers used in the present study were supplied by Bayer and Union Carbide, respectively. The weight average molecular weight $\bar{M}_w$ is 30,000 g/mol for PC and 120,000 g/mol for PCL.

The PC/PCL blends were prepared by melt extrusion after drying the PC in a vacuum oven at 373 K for 4 days. Thin ribbons of the blends were prepared after mixing the homopolymers in a laboratory scale screw extruder, at temperatures in the range 453–468 K in the die and 463–488 K in the barrel zone, depending on the composition. The temperatures employed for the preparation of the blends are too low for the occurrence of transesterification reactions between PC and PCL. This was verified by FTIR and both ^{1}H NMR and ^{13}C NMR and the results confirm that no chemical modification has taken place within the resolution of the spectroscopic experiments performed.

Two compositions, i.e. 90/10 and 80/20 were studied in addition to the PC homopolymer. DSC experiments on these extruded samples confirm that the components are forming an homogeneous amorphous mixture for these compositions with a single glass transition temperature intermediate between the homopolymers T_g.

Samples for BBDS and WAXS experiments were compression molded films prepared between stainless steel plates covered with a polyimide film (Kapton). These films were prepared directly from the freshly extruded samples. WAXS experiments established that the molding procedure did not change for these compositions the original amorphous state of the extruded ribbons.

2.2. WAXS experiments

Wide angle X-ray scattering (WAXS) experiments were performed in a Philips automatic diffractometer by using Cu Kα Ni filtered radiation, (40 kV, 40 mA). The spectra are recorded in an angular range $5° < 2\theta < 35°$ at a speed of 0.0133 °/s. The high temperature runs were performed in an Anton Paar high temperature camera, under a nitrogen atmosphere. The temperature stability was better than 0.1 K. Once T_c is reached, consecutive runs were programmed. The crystallinity degree (X_c) of the PC component was determined by a peak decomposition of the WAXS spectra which includes the PC crystalline peaks and the contributions from the PC and PCL amorphous phase. This latter contribution was evaluated from the intensity recorded on the initial run at 418 K when the blend is 100% amorphous by assuming that its profile does not change, only its intensity is modified during isothermal crystallization.

2.3. BBDS experiments

The BBDS experiments measuring the complex dielectric constant $\varepsilon^* = \varepsilon' - i\varepsilon''$ were performed in a Novocontrol Concept Twelve Spectrometer with frequencies ranging from 10^{-2} Hz to 3.16 MHz. The system is based on a Schlumberger frequency response analyzer (FRA SI 1260) with a broad band dielectric converter remote interface and a temperature controller which provides a stability of better than 0.1 K. The sample is located between two horizontal metallic electrodes and a permanent gaseous nitrogen flux is the exchange gas. The samples are disks 30 mm in diameter and 100 μm thick with sputtered gold electrodes. First, the three samples with compositions 100/0, 90/10 and 80/20 were studied over a wide temperature range, from 133 K up to 473, 443 and 373 K, respectively. Isothermal runs were performed every 5 K. Second, a crystallization temperature, T_c, was chosen which has to comply with several requirements: the main relaxation mode should be centered in the selected frequency window; the lowest frequency

should be high enough so as the time for the frequency sweep should be small as compared to the crystallization kinetics at the chosen working temperature. Temperatures of 408 and 418 K and frequencies ranging from 100 Hz to 3.16 MHz were used.

2.4. Analysis of dielectric results

The analysis of the dielectric spectra was carried out by decomposing the experimental trace of the imaginary part of the dielectric constant as a function of the angular frequency, $\varepsilon''(\omega)$, recorded at different temperatures, into up to three relaxation modes. Havriliak–Negami (H–N) distribution of relaxation times was used in the case of the main relaxation mode in the spectra. The contribution of the conductivity, σ_0, is added and taken as proportional to ω^{-1}. The experimental trace recorded at constant temperature, is thus fitted to the following expression [10].

$$\varepsilon''(\omega) = \sum_{k=1}^{3} \frac{\Delta\varepsilon_k \sin(\gamma_k \phi_k)}{[1 + 2(\omega\bar{\tau}_k)^{\alpha_k}\cos(\pi\alpha_k/2) + (\omega\bar{\tau}_k)^{2\alpha_k}]^{\gamma/2}} - \left(\frac{\sigma_0}{\varepsilon_0\omega}\right) \quad (1)$$

with

$$\phi = \tan^{-1}\left(\frac{(\omega\bar{\tau}_k)^{\alpha_k}\sin(\pi\alpha_k/2)}{1 + (\omega\bar{\tau}_k)^{\alpha_k}\cos(\pi\alpha_k/2)}\right) \quad (2)$$

and where ε_0 denotes the permittivity of free space and with $\Delta\varepsilon_k = (\varepsilon_s - \varepsilon_\infty)_k$ being the dielectric strength for the kth mode.

At each temperature a value of the mean relaxation time, $\bar{\tau}_k(T)$, is found for the modes present in the frequency window used here. The relaxation diagrams are plots representing the variation of $\log \bar{\tau}_k(1/T)$ which will be linear in the case of Arrhenius dependence for the relaxation time and curved for Vogel–Tammann–Fulcher, (VTF), ones according to their expressions:

$$\tau(T) = \tau_0 \exp[E_A/kT] \quad (3)$$

$$\tau_{VTF}(T) = \tau_{0VTF}\exp[E_{VTF}/k(T - T_0)] \quad (4)$$

τ_0 and τ_{0VTF} are the preexponential factors, E_A and E_{VTF} are characteristic parameters (eV) for the Arrhenius and VTF relaxation times, that describes the temperature dependence of the local and segmental relaxation, respectively.

The fitting procedure is complicated because of the presence, of very often incomplete peaks in the frequency window of more than 8 decades used here. As the temperature increases, the relaxation peaks shift to higher frequencies and sweep the frequency window.

3. Results and discussion

3.1. X-ray diffraction results

The extruded ribbons were found to be completely amorphous for blends with less than 40% in PCL weight. For the 50/50 blend the Bragg diffraction peaks characteristic of the PCL orthorhombic non-planar structure with space group $P2_12_12_1$ [11] are clearly visible. Fig. 1 illustrates the absence of any crystalline structure in the extruded samples for the compositions studied here.

The isothermal crystallization experiments were performed on the 90/10 PC/PCL amorphous blend at 418 K; each angular sweep lasted 38 min. In Fig. 2 selected runs are plotted where the X-ray reflections, due exclusively to the monoclinic structure of PC (space group Pc) [12], are clearly visible. The crystallization temperature chosen here is above the ideal melting temperature of PCL and no evidences on the formation of mixed crystals are detected. After 10 h most of the intensity variations observed in the WAXS spectrum have taken place. The crystallinity is now increasing at a very much-reduced rate for this temperature and composition. The plots in Fig. 3 represent the initial and final crystallization states reached after the isothermal annealings performed in the dielectric spectrometer at 408 and 418 K; the spectra are recorded at room temperature. Now that the time scale and the amount of the crystallization of the PC initially amorphous phase have been established, changes in the chain dynamics induced by the crystallization are studied in these same conditions.

3.2. Dielectric study of PC/PCL blends

The results for the dielectric losses obtained for pure PC and the PC/PCL blends with compositions 90/10 and 80/20 studied here are presented in Fig. 4(a)–(c) as $\varepsilon''(T)$ for $\nu = 1$ Hz, 100 Hz, 1 MHz, respectively. As expected for a miscible blend, there are clear differences between the

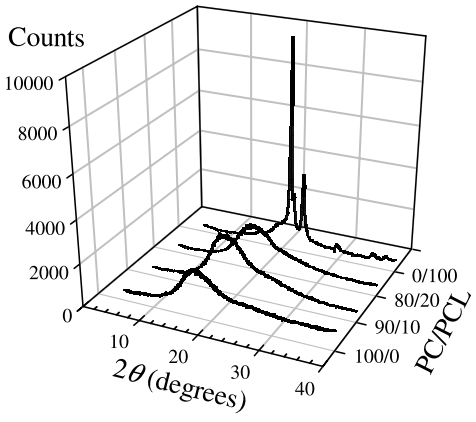

Fig. 1. Wide angle X-ray diffraction spectra for the extruded PC homopolymer, the 90/10 and 80/20 PC/PCL blends and the PCL homopolymer taken at 295 K with Cu Kα wavelength.

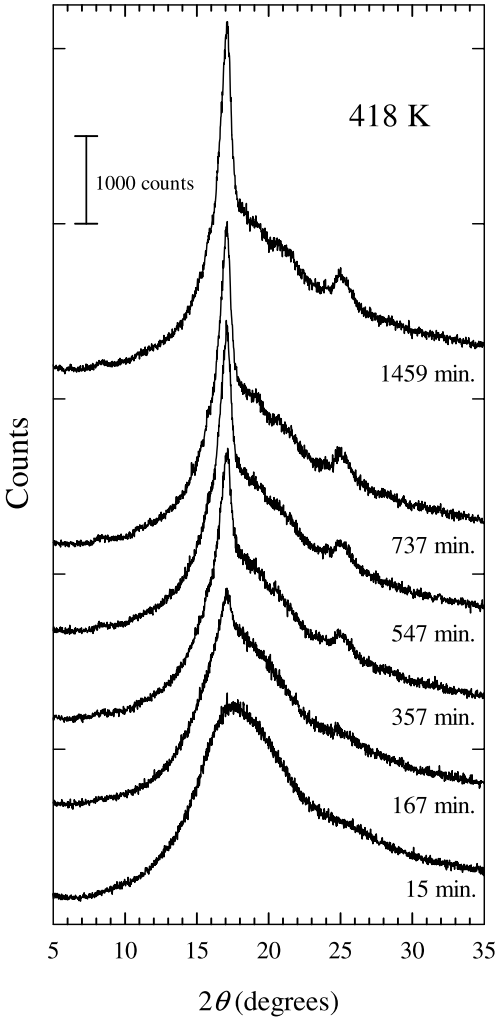

Fig. 2. Selected Wide angle X-ray diffraction spectra for the isothermal crystallization of the 90/10 PC/PCL blend at 418 K as a function of time. The time elapsed from the beginning of the experiment for each spectrum is indicated in the figure.

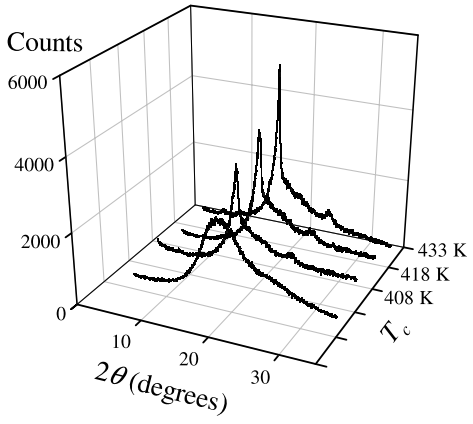

Fig. 3. Wide angle X-ray diffraction spectra of the 90/10 PC/PCL blend before and after isothermal crystallization in the dielectric spectrometer at 408, 418 and 433 K, spectra are recorded at room temperature.

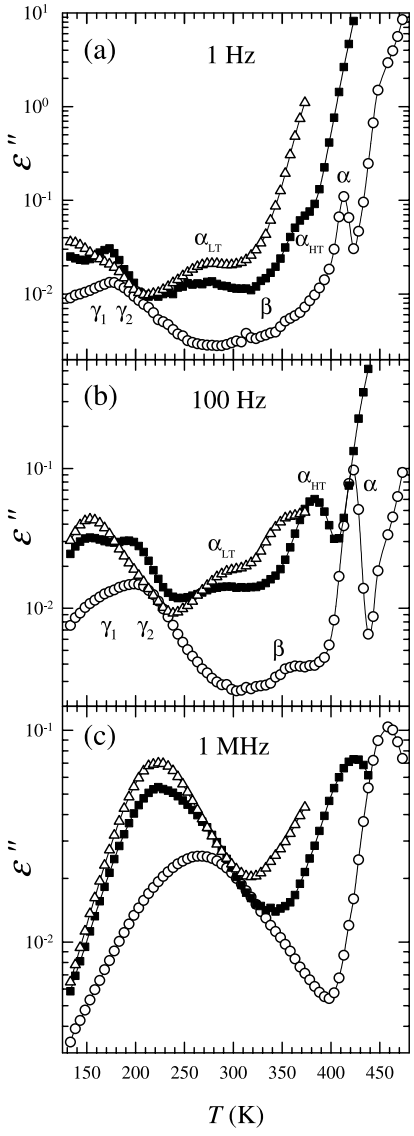

Fig. 4. Dielectric loss, $\varepsilon''(T)$ at constant frequency: (○) for the PC homopolymer, (■) the 90/10, and (△) the 80/20 PC/PCL blends for selected frequencies: (a) $\nu = 1$ Hz, (b) $\nu = 100$ Hz, (c) $\nu = 1$ MHz.

dielectric spectra of pure PC and its blends with PCL. The dielectric traces of pure PC clearly show the presence of a well-defined peak around 400 K, which corresponds to the dielectric manifestation of the dynamic glass transition, the α mode [13]. At 1 Hz the α mode appears on the rise of $\varepsilon''(T)$ associated to dc conductivity; at higher frequencies, as the peak shifts to higher temperatures, it becomes wider due to the overlap with a different relaxation process, which is labeled α'. This high temperature peak is very intense and has been related to the transport of free charges and further accumulation either on internal or external boundaries [14]. Additionally to these high temperature peaks, the secondary modes, γ_1 and γ_2, in pure PC appear as a very broad band which ranges from the low temperature limit of our dielectric experiments (133 K) up to 250 K at 1 Hz. In addition to these local modes a very weak sub-glass

transition, the β mode, is barely visible in the low frequency spectra (1 and 100 Hz) around 360 K.

When PCL is added to PC the dielectric isochrones show very distinct features from that of the PC homopolymer as seen in Fig. 4. The highest temperature region of the dielectric loss, $\varepsilon''(T)$, is dominated by dc conductivity or the merging of different processes [15] which start at temperatures lower than in the PC homopolymer. According to the Lodge–McLeish model the presence of two dynamic T_g's are expected due to the distinct effective concentrations around the chains of each blend component. The high temperature α mode, α_{HT}, appears as a shoulder in the conductivity rise at $\nu = 1$ Hz and is more visible at higher frequencies. As to the lower temperature α mode, α_{LT}, it could be assigned to the broad peak located in the β zone of PC, in the low temperature tail of the α_{HT} mode, where a steep increase of the signal is recorded as PCL concentration increases. The superposition of the β and α_{LT} modes with different temperature dependences for their relaxation times, explains the difficulty encountered in fitting this zone of the spectra in frequency domain, in order to extract the relaxation parameters. In addition, the profile of the composite local relaxation band changes as the PCL content in the blend grows.

The existence of two segmental dynamics and the significant shifts of the α_{HT} and α_{LT} relaxations, as the PCL content increases, indicates that in both PC/PCL amorphous blends each component has its own effective segmental mobility. These mobilities are distinct from that of the neat homopolymers and from that of the bulk mean value which is detected by DSC. A detailed analysis of the relaxation dynamics in these blends, to study the changes induced by the progressive PCL increase, will be performed by decomposing the isothermal traces, $\varepsilon''(\log(\nu))$, for the three PC/PCL compositions studied here. In Fig. 5(a)–(c) the isothermal $\varepsilon''(\nu)$ spectra for the PC/PCL blends studied are represented at temperatures where the main relaxation mode is visible. The spectra are decomposed in the contributions associated to the different relaxation modes present in the selected frequency zone. The conductivity contribution, σ_0, is subtracted from the total spectrum. In these figures, for the sake of clarity, only the α_{HT} mode resulting from the decomposition has been plotted (dashed line). In this way the profiles of the segmental modes for the homopolymer and the blends could be compared and the variation on the shape parameters and dielectric strength as PCL is added, followed. Also, from the result of the best fit of the isotherms, $\varepsilon''(\log(\nu))$, the average relaxation time for the main relaxation process is found at each temperature and the results are plotted as, τ_{HN} $(1/T)$, for the PC/PCL blends in Fig. 6. The experimental temperature dependence of τ_{HN} was fitted to the VTF equation, (Eq. (4)) for both blends and pure PC, confirming the cooperative character of the α and α_{HT} modes associated to the segmental mobility [16]. As shown in Table 1, by defining T_g as the temperature at which the dielectric τ is equal to 1 s, agreement is obtained with

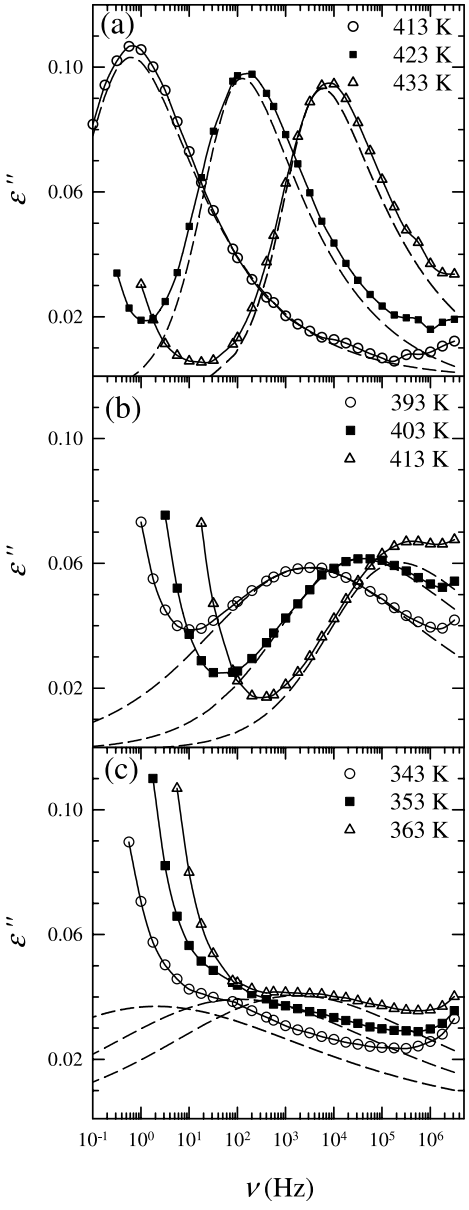

Fig. 5. Examples of the trace decomposition of $\varepsilon''(\nu)$ at selected temperatures: (a) PC homopolymer, (b) 90/10 PC/PCL blend, (c) 80/20 PC/PCL blend. Contributions from the low frequency conductivity have been subtracted; only the resulting α_{HT} profile is represented by a dashed line. The continuous line is the result of the fitting when all contributions have been added.

previous results from TSDC for the 80/20 blend [2]. The values of T_{VTF} are about 50 K lower than T_g as expected [16]. The observed VTF behavior in Fig. 6 shows the shift of τ_{HN} to higher values as T decreases, as the PCL content in the blends increases. This effect establishes the enhanced molecular mobility in the blends due to the plasticization of PCL over PC. The relaxation parameters for the VTF dependence of $\tau(T)$, E_{VTF} and τ_{0VTF}, are similar for the three materials; the only difference is in the position of this mode in the temperature axis, i.e. a difference both in T_g and T_{VTF}. It is worthwhile to note here that the only composition

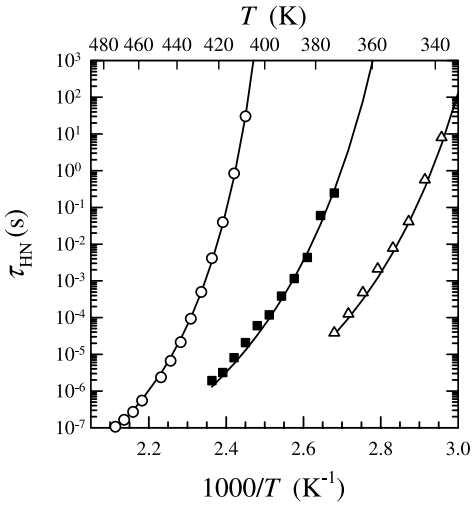

Fig. 6. Relaxation map, $\tau_{HN}(1/T)$, for the segmental mode: (○) α mode for the PC homopolymer, (■) α_{HT} for the 90/10, and (△) α_{HT} for the 80/20 PC/PCL blends. The lines are the fittings to the VTF equation which parameters are reported in Table 1.

dependent parameter in the VTF dependence of the segmental dynamics is the T_{VTF} temperature. This is the experimental proof that the hypothesis recently used [8,9] to calculate the VTF relaxation time variation with temperature is reasonable. It was assumed that among the VTF relaxation parameters, i.e. $\tau_{0VTF,i}$, $E_{VTF,i}$ (B_i/k in their notation) and $T_{0VTF,i}(\phi)$ for each component, only the last one was composition dependent and it represents the Vogel temperature for the i component.

The width and asymmetric shape of the relaxation mode are characterized by the α_{HN} and γ_{HN} parameters, respectively; their variations with temperature are represented in Fig. 7(a) and (b), against normalized temperature, T/T_g. The broadening of the blends relaxation mode is evidenced by the reduction in the α_{HN} parameter as the PCL concentration increases. Besides, as the temperature increases, a clear difference appears among these materials; both pure PC and the 90/10 PC/PCL blend show some degree of narrowing in their α_{HT} relaxation mode. On the

Table 1
Relaxation parameters for the α mode in PC/PCL blends

PC/PCL	α	
80/20	τ_{0VTF}(s)	$10^{(-11.3\pm0.6)}$
	E_{VTF}(eV)	0.11 ± 0.01
	T_{VTF}(K)	292 ± 3
	T_g[a](K)	342 ± 3
90/10	τ_{0VTF}(s)	$10^{(-12\pm1)}$
	E_{VTF}(eV)	0.13 ± 0.03
	T_{VTF}(K)	316 ± 10
	T_g[a](K)	369 ± 10
100/00	τ_{0VTF}(s)	$10^{(-12.9\pm0.5)}$
	E_{VTF}(eV)	0.12 ± 0.01
	T_{VTF}(K)	364 ± 3
	T_g[a](K)	413 ± 3

[a] The T_g values are calculated from the relaxation plot for $\tau(T_g)=1$ s.

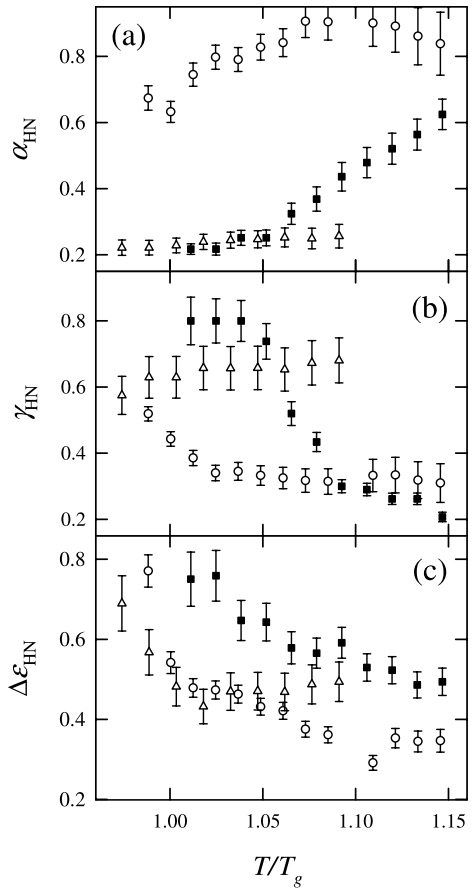

Fig. 7. Variation with reduced temperature of the HN parameters for the segmental relaxations: (○) for the PC homopolymer, (■) the 90/10, and (△) the 80/20 PC/PCL blends; (a) symmetrical broadening, (b) asymmetrical broadening, (c) dielectric strength.

contrary, the width of the segmental mode of the 80/20 PC/PCL blend is very large (close to 0.2) and remains nearly constant through the entire temperature interval. In miscible blends, the variation in the spectral broadening with temperature has been studied by Miura et al. [17] and Katana et al. [18] among others. These authors establish that the narrowing effect for the segmental mode as the temperature increases usually observed in homopolymers is not present in blends. They attribute the observed broadening to the presence of concentration fluctuations [17].

For the 80/20 blend the increase in the width of the segmental peak is so large that its definition in the frequency window used here is very poor as seen in Fig. 5(c). Moreover the low frequency rise observed in this same figure is predominant over the segmental peak. The errors assigned to the shape parameters of the 80/20 blend are consequently large and discussing the asymmetry and dielectric strength for this mode does not seem reasonable. The variation of the asymmetrical broadening with temperature, shown in Fig. 7(b) for the homopolymer and for the less PCL rich blend agrees with what one expects for amorphous polymers and super cooled liquids which present

an unsymmetrical and less broad relaxation peak for temperatures well above T_g [19], i.e. a Cole–Davidson distribution of relaxation times has often been found to be adequate. It is to be noted that the estimated errors in the shape factors determination are not large enough to modify the general trends reported on Fig. 7 as the temperature increases for PC and the 90/10 blend where the peaks under study are well defined.

Finally, the dielectric strength also shows differences as the blends become richer in PCL, as plotted in Fig. 7(c). Both pure PC and the two PC/PCL blends show the usual decrease in $\Delta\varepsilon$ as T increases above T_g in amorphous polymers [20]. This is caused by the decrease in the size of the rearranging regions of cooperative motion, CRR, [16] as the temperatures increases above T_g.

The strength increase when 10% of PCL is added to PC can be attributed to several causes: (a) the number of mobile dipoles increases simultaneously with the increase in their mobility due to the plasticization of PC by PCL; for example, if a constrained amorphous phase exists which would relax in the presence of PCL. (b) the Onsager–Kirkwood–Fröhlich g factor which reflects the orientation correlations between molecules could be different in the neat PC and in the 90/10 blend due to the extrusion procedure. However, the molding process at 513 K should have been sufficient to erase the preferential orientation.

All the evidence presented above establishes that the amorphous 90/10 and 80/20 PC/PCL blends are miscible with relevant concentration fluctuations that affect the behavior of the intensity, width and asymmetry of the cooperative α mode corresponding to the high T_g component. The understanding of the variation of these parameters needs a wider composition range and these studies are currently performed by TSDC and DSC techniques.

3.3. Dielectric studies during the isothermal crystallization of the 90/10 PC/PCL blend

PC in PC/PCL blends is known to exhibit an enhanced rate of crystallization with respect to pure PC, due to the PCL plasticization effect, and this morphological change seems to play an important role in the homogeneity of these blends [2]. The study of the isothermal crystallization of a 90/10 PC/PCL blend is possible by using BBDS and the results will help the understanding of the changes in the molecular dynamics as the crystallites develop. The kinetics of crystallization are studied by recording in real time the evolution of the dielectric spectra of the α process, for samples heated from the glassy state at room temperature up to T_c. The analysis of the cold crystallization in polymers by dielectric methods has been performed by several groups, specially in the case of rigid main chain crystallizable polymers, like PET [21] or PEEK [22], which can be obtained in a completely amorphous state by quenching from $T > T_g$ from the equilibrium supercooled state. As the motions in the amorphous phase are greatly affected by the formation of the crystallites, the crystallization process is easily detected. The crystalline phase growth is visualized through the decrease in $\Delta\varepsilon(t)$, which is proportional to the amount of mobile amorphous material at the crystallization time t. The mobile amorphous amount is formed by the amorphous chains which cooperatively reorient in the presence of an electric field. If the mobility of the whole amorphous phase is assumed, then, X_c, the volume fraction of the newly formed crystalline phase can be expressed as

$$X_c = 1 - [\Delta\varepsilon(t)/\Delta\varepsilon(0)] \quad (5)$$

Massalska-Arodz et al. [23] use an alternative way for estimating the degree of crystallinity in isooctyloxycyanobiphenyl, i.e. the decrease in the dielectric strengths ratio being taken as proportional to the ratio of the dielectric loss, $\varepsilon''(t)/\varepsilon''(0)$. The two ratios are proportional only if the profile of the α mode does not change through the crystallization process. In the blend system studied here, and in all the previous dielectric studies of in situ crystallization on various polymer systems, the spectral line shape of the segmental mode changes drastically as we shall discuss below.

Fig. 8(a) and (b) show the data for $\varepsilon''(\nu,t)$ for the crystallization of the 90/10 PC/PCL blend at 408 and 418 K, respectively. At both temperatures the WAXS experiments, see Figs. 2 and 3, indicate that crystallization develops in times compatible with the experimental time scale. Both Fig. 8(a) and (b) present similar features: at both crystallization temperatures the dielectric loss spectrum decreases in intensity up to a time where the α_{HT} mode is no longer distinguished in the relaxation spectrum. This final state is reached after 72 h at 408 K and 21.2 h at 418 K. Additionally, in the case of the lower crystallization temperature no relevant shift to lower frequencies of the ε'' maximum value is visualized as PC crystallizes. The exact changes in the dielectric strength and in the shape and position of the α_{HT} mode with crystallization time can be extracted by performing the similar detailed analysis described above, i.e. adjusting the relaxation spectra to a Havriliak–Negami distribution. In Fig. 9(a) and (b left axis, filled symbols) are represented the time evolutions of the dielectric strength, $\Delta\varepsilon(t)$ for $T_c = 408$ and 418 K, respectively. In both cases there is a large reduction in $\Delta\varepsilon(t)$ values, i.e. 58% at 408 K and 77% at 418 K which represent the amount of amorphous material which is now not contributing to the relaxation phenomena. The crystallinity degrees calculated for the 90/10 blends whose WAXS trace is reported in Fig. 3 are 17% for both crystallization temperatures. In Fig. 9 (b, right axis, empty symbols) the variation of the crystallinity degree as a function of time has been plotted. From the comparison of the two plots in this figure, it is readily seen that the primary crystallization takes place simultaneously with the disappearance of the entire mobile amorphous phase. This is an indication on the

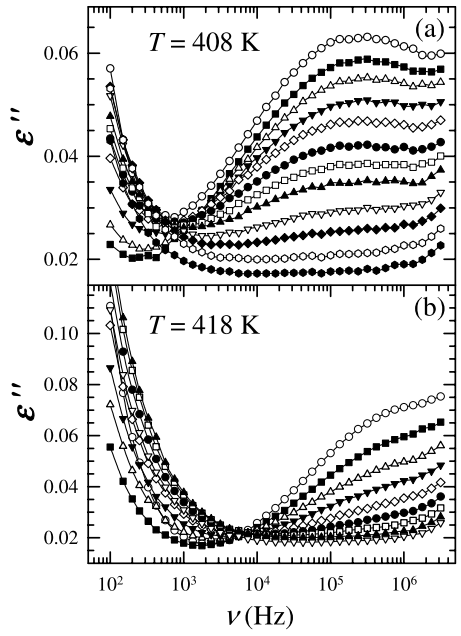

Fig. 8. Variation of the dielectric loss, $\varepsilon''(\nu)$, at selected times during isothermal crystallization for the 90/10 PC/PCL blend: (a) for T_c=408 K, (b) for T_c=418 K. Time is increasing from top to bottom.

parallel formation of the crystalline regions and an amorphous fraction which does not contribute to the segmental relaxation. After 10 h at 418 K the remaining mobile amorphous phase has reached its lowest value whereas the crystallinity is still growing at a lower rate. The filling of space with spherulites and the formation of a

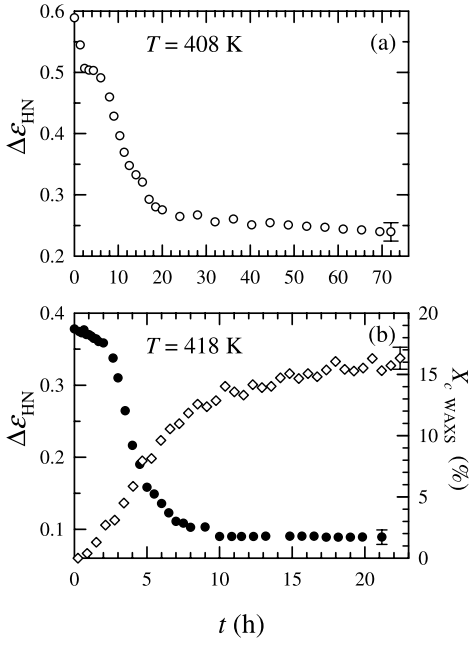

Fig. 9. Variation of the dielectric strength of the α mode as a function of the crystallization time in 90/10 PC/PCL blend calculated from the HN fitting of the dielectric loss spectrum: (a) for T_c=408 K, (b) for T_c=418 K; (◇) variation of the crystallinity degree, right axis. Typical error bars are indicated.

constrained amorphous phase occur during the same time scale. After this crystallization time of about 10 h, the slight changes observed in the crystallinity do not affect the strength of the dielectric α mode. The large discrepancy observed between the relative decrease of the dielectric α relaxation strength, associated with the reorientable segmental population, and the crystalline material obtained from WAXS measurements indicates that the disappearance of the mobile amorphous phase is not only coupled to the crystalline growth visible by WAXS. As the primary crystallization progresses, only a small fraction of the remaining amorphous phase is able to perform the segmental motions characteristic of the α relaxation. The loss of mobile amorphous phase estimated after dielectric measurements minus the relative amount of crystalline material has been rationalized as the rigid amorphous fraction. The topological constraints imposed by crystal formation results in chain stiffness effects that hinders the segmental mobility. This effect has been reported previously in cold crystallization processes followed by dielectric measurements in PEEK by Nogales et al. [24], in PEKK by Ezquerra et al. [25] and by TSDC measurements in crystalline BAPC by Laredo et al. [13]. The existence of a rigid amorphous fraction was originally proposed to explain the discrepancies between the theoretical and experimental heat capacity changes at T_g, ΔC_p, determined by differential scanning calorimetry [26,27]. This constrained amorphous phase would be able to attain the characteristic mobility of the supercooled liquid well above T_g near the melting region, remaining immobile at temperatures around the glass transition. Several others works have reported discrepancies between the total amount of amorphous material and the mobile fraction capable of segmental motion in partially crystalline polymers [28–30]. A general understanding of this behavior is still lacking, but the presence of immobile amorphous chains in partially crystalline polymers has been frequently associated to the presence of irregular interfaces between crystalline and amorphous phase at a nanometer scale, resulting from interfacial strains that concentrates at the crystalline lamellae boundaries [31].

The evolution of the shape parameters of the HN distribution during isothermal crystallization is reported in Fig. 10(a) and (b) for T_c=408 and 418 K, respectively, and their behavior is very similar. The width of the distribution increases as the α_{HN} parameter varies from 0.44 to 0.2 or from 0.55 to 0.3 for the higher crystallization temperature. This parameter is related to the long range motions connected with intermolecular interactions [32] and its decrease in the early crystallization stages evidences the strong effect of the 3D order formation on the segmental dynamics. On the contrary, the asymmetrical parameter, γ_{HN}, levels off at its maximum allowed value of 1, as shown in these figures, at times where the crystallites have nearly fully developed as seen by the decrease in the $\Delta\varepsilon_{HN}$ values. This is an interesting result as the loss of asymmetry in the

relaxation time distribution when the fully amorphous state is lost justifies the use of Cole–Cole distributions for the analysis of the segmental mode in semicrystalline polymers. In Fig. 10 the variations of the product $\alpha_{HN}\gamma_{HN}$ are also plotted and their changes are very small over the entire time range. This product has been related by Schlösser and Schönhals [32] to the intramolecular interactions which mainly affect the short range chain dynamics. The smooth variation of this product establishes the weak effect of the crystallization upon the small scale motions which contribute to the α_{HT} mode.

The results of the fitting of the dielectric spectra $\varepsilon''(\nu,t)$ reveal other important features for PC crystallization in the 90/10 PC/PCL blend and its effect on the dynamics of the segmental motion. Fig. 11(a) and (b), empty symbols, represent the variation of the relaxation time measured at the maximum loss, τ_{Max}, of the α_{HT} mode as a function of crystallization time for both crystallization temperatures. It has been extensively argued that crystallization hinders the overall mobility of chain segments in the amorphous phase attached to the crystals [33]. However, the magnitude of the slowering of the motion is variable and depends on several factors such as the crystallization time and temperature, and mainly the polymer structure and morphology. Polymers like PEEK [34] show an increase in τ_{Max} by a 100 factor. Other polymers like PEKK [25] or low molecular weight compounds [35] reveal a more discrete evolution of less than a decade after complete crystallization. Finally, in copolymers like P(HB-*co*-HV) [36] or block copolymers like PBT-*b*-PC [37] no differences are observed between the values of τ_{Max} in the amorphous sample and after cold crystallization. Comparing PC crystallization at 408 and 418 K for the 90/10 PC/PCL blend, it is observed that the

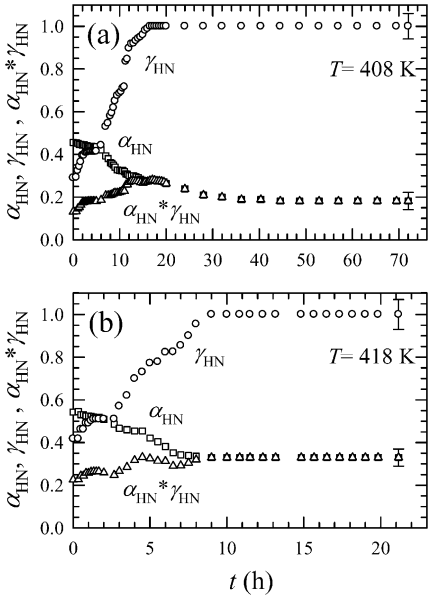

Fig. 10. Variation for the 90/10 PC/PCL blend of the HN relaxation parameters: (○) γ_{HN}, (□) α_{HN}, (△) $\alpha_{HN}\gamma_{HN}$: (a) for T_c=408 K, (b) for T_c=418 K. Typical error bars are indicated.

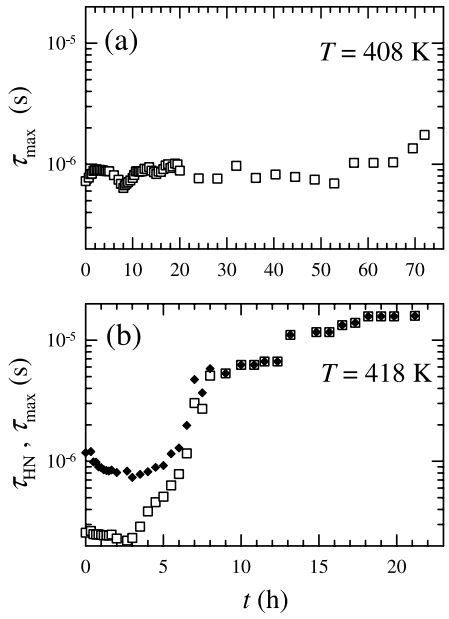

Fig. 11. Variation for the 90/10 PC/PCL blend of the relaxation time at the loss maximum (empty symbols), τ_{max}, and its average in the HN model: (a) for T_c=408 K, (b) for T_c=418 K; τ_{HN}, as a function of time (filled symbols).

τ_{Max} variation becomes more relevant as T_c increases, indicating that the effect of crystallization on segmental dynamics increases with crystallization temperature. At the lowest T_c studied here, the average dynamics of the α relaxation is nearly unaffected by crystallization. By contrast, at 418 K, the significant increase of τ_{Max} by a factor of 50, indicates that the constraints imposed by the crystallization process on the segmental mobility are very important. As it has been shown in the previous section for amorphous samples, the main effect of the addition of PCL to the PC phase is the increase in the segmental mobility as a result of plasticization. In fact, a consequence of this plasticization is that the PC cold crystallization occurs during the experimental time scale used here. Thus, the differences observed at both crystallization temperatures can be related to the competing effects due both to the PCL plasticization effect and to the level of constraints imposed by the PC new morphology (i.e. lamellae and rigid amorphous phase) over the mixed mobile amorphous phase. Since, there is no evidence of phase separation during PC crystallization, the development of a phase of pure PC crystals, necessarily, must result in a PCL enrichment in the mixed amorphous phase, resulting in more plasticization that compensates the effects of the crystallization process. In previous works, on P(HB-*co*-HV) copolymers [36],the invariance of τ_{Max} as the crystallization progresses has been associated to the absence of an efficient secondary crystallization process, which has been proposed as responsible for the restrictions of the crystals over the segmental dynamics of the amorphous phase [38]. In Fig. 11 (b, filled symbols) the variation of $\tau_{HN}(t)$ has been added.

Even though the traces of $\tau_{HN}(t)$ and τ_{Max} (t) are significantly different at the initial crystallization state, they merge as the crystallization advances. This is another evidence on the transition from an asymmetric to a symmetric relaxation time distribution as the initially amorphous polymer crystallizes.

It is worth noting that Fukao et al. [21] have proposed a different interpretation of the changes observed by dielectric measurements on the α mode during crystallization. In isothermal cold crystallization studies in PET, these authors have proposed a dynamic transformation of the α mode, associated to the glass transition, into another relaxation, α', which coexists with the first during crystallization and finally prevails over the α mode. All these modifications occur before observable 3D order will be detected in X-ray scattering patterns. In our case there exists also a significant change in the $\varepsilon''(\nu,t)$ low frequency tail as can be seen in Fig. 8. After a steep initial decrease in the signal intensity at the lowest border of our experimental frequency window, the intensity tail grows steadily during crystallization. This tail is attributed to the effect of both the dc conductivity contribution and to the development of an α' mode due to the formation of an interfacial polarization as the crystalline lamellae develop. If there is a second dynamical process slower than the α mode hidden under this tail, it would be very difficult to extract due to the other contributions which are very intense.

Wurm et al. [39] propose a different experimental approach to study dielectrically the early stages of crystallization. The development of additional interfaces would result in a Maxwell–Wagner–Sillars polarization different from electrode charge accumulation in supercooled equilibrated melts. This effect is best observed in the traces of the real part of the dielectric constant, $\varepsilon'(\nu,t)$ where a maximum occurs at the early crystallization times. In our case the frequency window selected here is not wide enough to follow this possible effect and complementary work is carried on at this time.

3.4. Crystallization kinetics of the 90/10 PC/PCL blend

We have tried to fit the dielectric data plotted in Fig. 9(b) to the Avrami equation [40,41]:

$$X_c(t) = 1 - \exp(-Kt^n) \tag{6}$$

where $X_c(t)$ is the relative crystalline fraction of the polymer as a function of time. The parameters K and n are dependent on the nucleation type and the crystal growth geometry, K can be considered an overall transformation rate constant and n is the Avrami index. In order to apply the equation, the reduction in the amorphous phase mobility (as determined by reduction in the dielectric strength of the α mode) has to be considered as exclusively related to the crystallization of the material (Eq. (5)). In other words, the possible formation of a rigid amorphous phase has to be ignored.

The Avrami equation was only able to describe the data for a restricted relative conversion to the crystalline state of approximately 3–20% and an Avrami index of approximately 2 was obtained. This result does not represent the physical events during crystallization since optical microscopy experiments have shown for the 90/10 PC/PCL blend the presence of spherulites. Furthermore, the long induction times for crystallization are consistent with sporadic nucleation, therefore an Avrami index of 4 was expected. We believe that the reason behind the failure of the Avrami equation to represent the collected data is due to the formation of the PC rigid amorphous phase. While the final degree of crystallinity obtained after isothermal crystallization at 418 K was 17%, the amount of amorphous phase that fails to contribute to the α primary relaxation is around 70%. Therefore, the data from Fig. 9(b) cannot be converted to relative crystalline fraction without the knowledge of the amount of amorphous phase that is transformed into crystals as a function of time, or without a detailed knowledge of the rigid amorphous phase appearance kinetics.

Finally, an attempt was made to apply the Avrami equation to the WAXS data presented in Fig. 8. Even if the quality of the fit improved, the results once more were not satisfactory since an Avrami index of 2.2 was obtained. The Avrami equation describes the progressive transformation of a liquid to a crystal taking into account nucleation and growth dimensionality. Since in the present case liquid PC transforms into two different phases (crystalline and rigid amorphous), a kinetic model that takes into account this type of complex condensation would be more appropriate. We conclude that the crystallization of PC within the PC/PCL blend studied here is a very complex process that is affected by the simultaneous formation of a rigid amorphous fraction and therefore cannot be described by a simple kinetic treatment such as described by the Avrami equation.

4. Conclusions

The segmental dynamics in the extruded samples for the 100/0, 90/10 and 80/20 PC/PCL blends which are 100% amorphous, show the plasticization effect of the PCL. The cooperative mode thoroughly analyzed here corresponds to the high T_g component segmental dynamics of the self-concentration model for miscible blends [7]. The relaxation parameters extracted from the HN relaxation time distribution as a function of temperature show the following characteristics as the PCL content increases: (a) the relaxation times have a VTF energy and preexponential factor which remain approximately constant, but there is a strong decrease in the VTF temperature, (b) the profile of the HN distribution is much wider for the blends than for the homopolymer which points to the existence of increasing local heterogeneities in the homogeneous blends.

The comparative real time studies by WAXS and BBDS

on the polycarbonate rich PC/PCL blends lead to a better knowledge of the crystallization process either by recording the growth of the crystalline X-ray reflections or by following the decrease in the dielectric strength of the blend primary relaxation mode as a function of time. The isothermal crystallization as seen from the decreasing dielectric strength of the α_{HT} mode and the increase in the intensity of the Bragg peaks due to the crystalline PC component show that a two phase model is inadequate. A three phase model where a constrained amorphous phase forms by the time that the blend is undergoing its primary crystallization agrees better with the results found here. This constrained amorphous phase which does not contribute to the number of relaxing entities originating the α mode, is more important at 418 K than at 408 K. Its formation is simultaneous with the 3D ordering of the PC. The relaxation dynamics of the mobile PC chains at 408 K is unaffected by the combined effect of the PCL plasticization effect and by the rigidization of the PC as crystallization progresses. However, at 418 K, where the amount of rigid amorphous phase is more important, the segmental mobility is slowed down indicating that the rigidization effect is predominant on the plasticization even though the X_c final value is the same at the two temperatures. The more abundant rigid amorphous phase at 418 K also constrains the amorphous material able to undergo cooperative motions. On the morphology of this immobile fraction, one may propose that it could include an amount of crystal precursors which are too imperfect to contribute either to the 3D order detected by WAXS nor to the cooperative relaxation of the amorphous chains. Finally, we have found that the Avrami equation does not provide a suitable description of the crystallization kinetics experienced by this three phase material which develops in PC/PCL blends rich in PC as isothermal crystallization progresses.

Acknowledgements

We thank J.C. Zamora for providing the extruded samples. This work is part of Project G97-000594, FONACIT, and we thank them for their financial support.

References

[1] Balsamo V, Calzadilla N, Mora G, Müller AJ. J Polym Sci, Part B: Polym Phys 2001;39:771.
[2] Hernandez MC, Laredo E, Bello A, Carrizales P, Marcano L, Balsamo V, et al. Macromolecules 2002;35:7301.
[3] Cruz CA, Paul D, Barlow JW. J Appl Polym Sci 1979;23:589.
[4] Cheung YW, Stein RS, Wignall GD, Yang HE. Macromolecules 1993;26:5365.
[5] Cheung YW, Stein RS. Macromolecules 1994;27:2512.
[6] Cheung YW, Stein RS. Macromolecules 1994;27:3589.
[7] Lodge TP, McLeish TCB. Macromolecules 2000;33:5278.
[8] He Y, Lutz TR, Ediger MD. J Chem Phys 2003;119:9956.
[9] Haley JC, Lodge TP, He Y, Ediger MD, von Meerwall ED, Mijovic J. Macromolecules 2003;36:6142.
[10] Bello A, Laredo E, Grimau M. Phys Rev B 1999;60:12764.
[11] Hu H, Dorset DL. Macromolecules 1990;23:4604.
[12] Bonart R. Makromol Chem 1966;92:149.
[13] Laredo E, Grimau M, Müller A, Bello A, Suarez N. J Polym Sci, Part B: Polym Phys 1996;34:2863.
[14] Schönhals A, Kremer F. In: Schönhals A, Kremer F, editors. Broad band dielectric spectroscopy. Berlin: Springer; 2003. p. 87.
[15] Grimau M, Laredo E, Perez MC, Bello A. J Chem Phys 2001;114: 6417.
[16] Gibbs JH, DiMarzio EA. J Chem Phys 1958;28:373.
[17] Miura S, MacKnight WJ, Matsuoka S, Karasz FE. Polymer 2001;42: 6129.
[18] Katana G, Fischer EW, Hack Th, Abetz V, Kremer F. Macromolecules 1995;28:2714.
[19] Angell CA, Ngai KL, McKenna GB, McMillan PF, Martin SW. J Appl Phys 2000;88:3113.
[20] Schönhals A. In: Runt JP, Fitzgerald JJ, editors. Dielectric spectroscopy of polymeric materials. Washington, DC: American Chemical Society; 1997. p. 81.
[21] Fukao K, Miyamoto Y. Phys Rev Lett 1997;79:4613.
[22] Nogales A, Ezquerra TA, Batallán F, Frick B, López-Cabarcos E, Baltá-Calleja FJ. Macromolecules 1999;32:2301.
[23] Massalska-Arodz M, Williams G, Thomas DK, Jones WJ, Dabrowski R. J Phys Chem B 1999;103:4197.
[24] Nogales A, Ezquerra TA, Denchev Z, Šics I, Baltá-Calleja FJ, Hsiao B. J Chem Phys 2001;115:3804.
[25] Ezquerra TA, Majszczyk J, Baltá-Calleja FJ, López-Cabarcos E, Gardner KH, Hsiao BS. Phys Rev B 1994;50:6023.
[26] Suzuki H, Grebowicz J, Wünderlich B. Br Polym J 1985;17:1.
[27] Cheng SZD, Wünderlich B. Macromolecules 1988;21:789.
[28] Xu H, Cebe P. Macromolecules 2004;37:2797.
[29] Kalika DS, Wu SS, Lamonte RR, Makhija S. J Macromol Sci-Phys B 1996;35:179.
[30] Huo P, Cebe P. Macromolecules 1992;25:902.
[31] Cheng SZD, Wu ZQ, Wünderlich B. Macromolecules 1987;20:2802.
[32] Schlösser E, Schönhals A. Colloid Polym Sci 1989;267:133.
[33] Coburn JC, Boyd RH. Macromolecules 1986;19:2238.
[34] Ezquerra TA, Liu F, Boyd RH, Hsiao BS. Polymer 1997;38:5793.
[35] Dobbertin J, Hannemann J, Schick CJ, Pötter M, Dehne H. Chem Phys 1998;108:9062.
[36] Šics I, Ezquerra TA, Nogales A, Baltá-Calleja FJ, Kalninš M, Tupureina V. Biomacromolecules 2001;2:581.
[37] Ezquerra TA, Roslaniec Z, López-Cabarcos E, Baltá-Calleja FJ. Macromolecules 1995;28:4516.
[38] Alizadeh A, Sohn S, Quinn J, Marand H, Shank LC, Iler HD. Macromolecules 2001;34:4066.
[39] Wurm A, Soliman R, Schick C. Polymer 2003;44:7467.
[40] Schultz J. Polymer crystallization. Washington: American Chemical Society; 2001.
[41] Avrami M. J Chem Phys 1939;7:1103. Avrami M. J Chem Phys 1940; 8:212. Avrami M. J Chem Phys 1941;9:177.